J Mater Sci: Mater Med (2017)28:61
DOI 10.1007/s10856-017-5866-y

DELIVERY SYSTEMS

Original Research

Extended pulsated drug release from PLGA-based minirods

Y. Danyuo[1,2] · O. E. Oberaifo[3] · J. D. Obayemi[1,4] · S. Dozie-Nwachukwu[1,3] · C. J. Ani[5,6] · O. S. Odusanya[3] · M. G. Zebaze Kana[2] · K. Malatesta[7] · W. O. Soboyejo[1,4,7]

Received: 27 October 2016 / Accepted: 7 February 2017

Abstract The kinetics of degradation and sustained cancer drugs (paclitaxel (PT) and prodigiosin (PG)) release are presented for minirods (each with diameter of ~5 and ~6 mm thick). Drug release and degradation mechanisms were studied from solvent-casted cancer drug-based minirods under in vitro conditions in phosphate buffer solution (PBS) at a pH of 7.4. The immersed minirods were mechanically agitated at 60 revolutions per minute (rpm) under incubation at 37 °C throughout the period of the study. The kinetics of drug release was studied using ultraviolet visible spectrometry (UV-Vis). This was used to determine the amount of drug released at 535 nm for poly (lactic-co-glycolic acid) loaded with prodigiosin (PLGA-PG) samples, and at 210 nm, for paclitaxel-loaded samples (PLGA-PT). The degradation characteristics of PLGA-PG and PLGA-PT are elucidated using optical microscope as well as scanning electron microscope (SEM). Statistical analysis of drug release and degradation mechanisms of PLGA-based minirods were performed. The implications of the results are discussed for potential applications in implantable/degradable structures for multi-pulse cancer drug delivery.

Electronic supplementary material The online version of this article (doi:10.1007/s10856-017-5866-y) contains supplementary material, which is available to authorized users.

✉ W. O. Soboyejo
soboyejo@princeton.edu

[1] Department of Materials Science and Engineering, African University of Science and Technology (AUST), Abuja, Federal Capital Territory, Nigeria

[2] Department of Materials Science and Engineering, Kwara State University, Ilorin, Nigeria

[3] Biotechnology and Genetic Engineering Advanced Laboratory, Sheda Science and Technology Complex (SHESTCO), Abuja, Federal Capital Territory, Nigeria

[4] Department of Mechanical and Aerospace Engineering 41 Olden Street, Princeton University, Princeton, NJ 08544, USA

[5] Department of Theoretical Physics, African University of Science and Technology (AUST), Abuja, Federal Capital Territory, Nigeria

[6] Department of Physics, Salem University, Lokoja-Ajaokuta Road, Lokoja, Kogi, Nigeria

[7] Princeton Institute for the Science and Technology of Materials (PRISM), Princeton University, 70 Prospect Street, Princeton, NJ 08544, USA

1 Introduction

In recent years, the increasing incidence of cancer has been associated with high cancer mortality rates across the globe [1]. In 2008, the World Health Organization (WHO) estimated all global deaths arising from cancer to be ~84 million [2]. The different types of cancers give rise to more deaths than those due to HIV/AIDS, tuberculosis and malaria [3]. Early detection and improved treatment are crucial for the successful management of cancer [4–7]. However, it is difficult to detect breast cancer at the early stages [8]. This often results in late detection, and a much lower probability of effective treatments especially when metastatic conditions are reached before detection.

The current cancer treatment methods, such as bulk systemic chemotherapy [9–12] and radiotherapy [13, 14], have severe side effects. Such side effects can be reduced by a sustained and controlled release of cancer drugs into regions containing cancer cells [15, 16]. There is, therefore,

Published online: 01 March 2017

a strong interest in localized cancer delivery from an implantable drug delivery systems [12, 15–19]. Prior work focused on the development of implantable non-resorbable systems for cancer drug delivery [12, 18]. However, such systems remain in the body, or require surgical removal, after drug release. There is, therefore, a need for bioresorbable structures for the localized and controlled release of cancer drugs [19–22].

Biodegradable microparticles have been formulated from poly(lactic-acid) (PLA) or poly(lactic-co-glycolic-acid) (PLGA) for controlled drug release [23, 24]. PLA or PLGA have also been shown to be biocompatible and biodegradable [25, 26]. By altering their molecular weights, sample sizes and surface morphologies [27], well-defined degradation rates can be achieved for control release of encapsulated therapeutic agents. There has been an increasing interest to study the release of drugs from minirods [28]. The current work explored the formation of paclitaxel^{TM} (PT) and prodigiosin (PG) encapsulated bioresorbable PLGA minirods. Different compositions/ratios of PLGA were used in the formation of the drug-based PLGA minirods.

2 Materials and methods

2.1 Materials

PLGA with different ratios of lactide to glycolide; 50:50 (Mw = 30,000–60,000), 65:35 (Mw = 40,000–75,000), 75:25 (Mw = 66,000–107,000) and 85:15 (Mw = 75,000–120,000) were procured from Sigma Aldrich (St Louis, MO,USA). Anti-cancer drug, paclitaxel^{TM}(PT) was procured from LC Laboratories (Woburn, MA, USA), while prodigiosin (PG) (a locally synthesized anti-cancer drug) was previously synthesized [29]. Dimethyl sulfoxide (DMSO), dichloromethane (DCM) and polyvinylpyrrolidone (PVP) were procured from BDH Chemicals (Poole Dorset, England).

2.2 Formation of PLGA-based minirods

The working concentrations of drugs (PG and PT) were obtained at 2.5 mg/ml as earlier presented [29]. In the formation of the minirods, two samples were prepared from 1 g of PLGA (50:50), dissolved with 1 ml DCM each in an airtight plastic container for 15 min. The samples were then stirred gently with a spatula until a homogeneous polymer-blend was formed. This procedure was then repeated for PLGA (65:35, 75:25 and 85:15). In forming the degradable minirods, 1 ml of drug solutions (2.5 mg/ml of PG or PT) were separately transferred to the PLGA polymer-blends to form PLGA-PG and PLGA-PT formulations. The polymer-drug mixtures were uniformly mixed. Subsequently, 1 ml of PVP stock solution (0.2 g/ml of PVP:DCM) was added to PLGA-PG/PLGA-PT as a cross-linker. The resulting mixtures were then mixed vigorously to form PLGA-PG-PVP or PLGA-PT-PVP. The blended samples were casted into molds. The casted samples were then compressed at ~250 N/m^2 on the surfaces of the molds to form devices with diameters of ~5 mm and thicknesses of ~6 mm. The samples were air dried at room temperature (29 °C) for 12 h before they were remolded. Molded samples were then subsequently dried at 40 °C under vacuum for 2 h (GALVAC vacuum oven, LTE Scientific Ltd., Greenfield State, USA).

2.3 Characterization of samples

Prior to optical imaging, the samples were washed thoroughly with distilled water to remove soluble products, salts or other impurities. They were then dried under vacuum conditions until a constant weight was achieved. Proscope HR 640 microscope (Bodelin Technologies, Oswego, NY, USA) and a scanning electron microscope (SEM) (ASPEX 3020, ASPEX Corperation, OR, USA) were used to observe and monitor structural changes during degradation process.

Ultraviolet visible spectroscopy (UV-Vis) system (CECIL 7500 Series, Buck Scientific Inc., East Norwalk, CT, USA) was carried out at different stages during the drug release and degradation experiment to characteriz the drugs released. This was done at a wavelength of 535 nm for PLGA-PG samples, and at 210 nm for PLGA-PT samples.

The thermal properties were measured using a Differential Scanning Calorimeter (DSC) (500A Series, Sno. 20130626094, Japan). The glass transition temperatures (T_g), crystallization temperatures (T_c), as well as the melting temperatures (T_m) were determine for all the prepared drug-polymer samples. Five milligrams of each sample were heated at 10 °C/min, from room temperature to 200 °C, with nitrogen supplied at a flow rate of 50 ml/min. The flow of nitrogen was maintained to establish an oxygen-free atmosphere. Thermal properties were then obtained after complete DSC scans.

2.4 Degradation and drug release

2.4.1 Polymer degradation

The initial masses of the samples were determined before incubation in glass test tubes containing 5 ml of PBS (pH 7.4). Drug release and hydrolytic degradation were carried out simultaneously in a digital incubator shaker (Innova 4300, New Brunswick Company Inc., NJ, USA) at 60 revolutions per min (rpm) at 37 °C. This environment was used to apply physiological conditions during localized drug delivery. Polymer degradation was also characterized

by weight loss (under in vitro conditions in PBS). The weight changes were determined from:

$$\frac{M_t}{M_i} = k\sqrt{t}, \tag{1}$$

where M_t is the mass of the sample at time t, M_i is the initial mass of the sample, t is the degradation time, and k is the degradation rate. The rate of polymer erosion was also determined from the absorption of PBS over duration of 2–6 months. These were given by:

$$\frac{dM}{dt} = -k \tag{2}$$

where dM is the change in mass at time, t and k is the kinetic rate constant of erosion.

2.4.2 Determination of drug release

The release of incorporated therapeutic agents were characterized using UV-Vis measurements over regular time intervals. Five milliliter PBS were changed regularly at 7 day-interval until the samples were fully degraded. The amount of drug released was determined with the UV-Vis at 7 days interval. Also, the rate of drug release was estimated from the reaction kinetics [30]. This gives;

$$\frac{dC}{dt} = -kC^n, \tag{3}$$

where k is the reaction rate constant, n is the order of drug release and C is the concentration of drug released at time t. Drug loading content (DL %) and the drug encapsulation efficiency (DEE %) are given, respectively, by [31]:

$$DL\% = W_d/(W_d + W_p) \times 100 \tag{4a}$$

and

$$DEE\% = (W_d/W_i) \times 100, \tag{4b}$$

where W_d is the amount of drug loaded, W_i is the initial mass of drug and W_p is the mass of the polymer incorporated. The effect of the average molecular weight change (due to the presence of PBS/moisture) causes hydrolytic degradation. This is given by [32]:

$$M_n' = \frac{M_n}{[1 + x(M_n/1800)]}, \tag{5}$$

where M_n is the initial average molecular weight of the sample, M_n' is the average molecular weight after reaction with PBS, and x is the moisture content (weight %).

2.4.3 Fluid diffusion in PLGA

The time-dependent power law equation for systems in which diffusion occurs within the polymeric networks was given by Peppas et al. [33] to be:

$$\frac{m_t}{m_i} = 4\left(\frac{D}{\pi\delta^2}\right)t^n = kt^n, \tag{6}$$

where m_t/m_i is the fraction of drug release, k is the geometric constant of the release system, n is the drug release exponent, depicting the release mechanism, δ is the thickness of the sample and D is the coefficient of diffusion. The constants k and n were obtained from the linear form of Eq. 6 as previously described [34].

3 Results

3.1 Statistical analysis

Statistical analysis for data were carried out for at least at three independent times and the average values ± standard errors (SE) were reported [35]. The present data were analyzed with Minitab software package (Minitab16, Minitab Inc., State College, PA, USA). Significance of the result were determined from the difference in the means. Paired t-test of variance (ANOVA) was used to analyze the effect of polymer ratio on the cumulative cancer drug release as well as the drug loading content. The pair t-test determine whether the differences between the paired samples differs from zero/target value [36]. The data were correlated with each other. Moreover, one sample z-test was employed to determine the effect of degradation on the pore dominants in PLGA-based minirods with respect to polymer ratio and incubation time. Z-test was found to be appropriate since the sampling method was a simple random sampling and the samples were independent from a defined population. In addition, one-sample t-test was used to determine the rate of mass loss in PLGA-based minirods. The one-sample t-test usually estimates the mean of a population and compare it to a target or reference value especially when the standard deviation of the population is unknown. Samples were evaluated with a one-tailed probability distribution (normal) plots. P-values ≥ 0.05 were found to be statistically significant unless otherwise affirmed.

3.2 Characterization and morphological changes

Optical micrographs of drug loaded PLGA-based minirods are presented for PT and PG loaded. A systematic differences between both agents (PT and PG) loaded in these structures are presented (Fig. 1a–c). Generally, the optical images of the samples revealed micro and macro voids on the surfaces and within the matrices with increasing degradation time (Fig. 1b (PG, PT) and 1c (PG)). The samples loaded with PT were hard and brittle and therefore cracked easily with increasing incubation time in PBS.

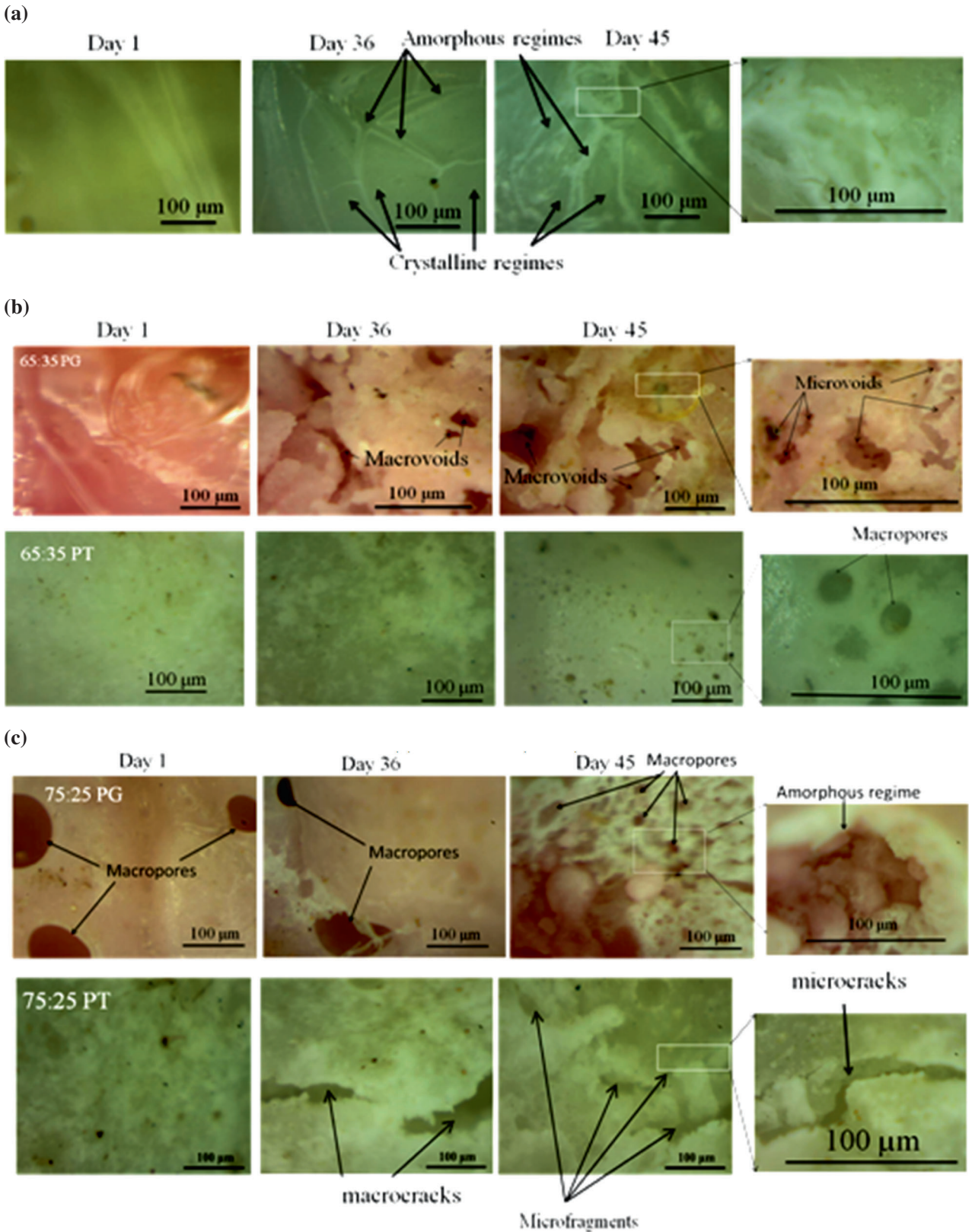

Fig. 1 **a–c** Optical microscopy images of PLGA-based minirods during degradation and drug release at 37 °C, pH 7.4, 60 rpm; **a** Control sample with no drug loaded, **b** PLGA 65:35 minirods loaded with PT and PG, respectively and **c** PLGA 75:25 minirods loaded with PT and PG, respectively. **d** PLGA (65:35) **e** PLGA (85:15). **d–e** SEM images of PLGA-based minirods during degradation and drug release at 37 °C, pH 7.4, 60 rpm

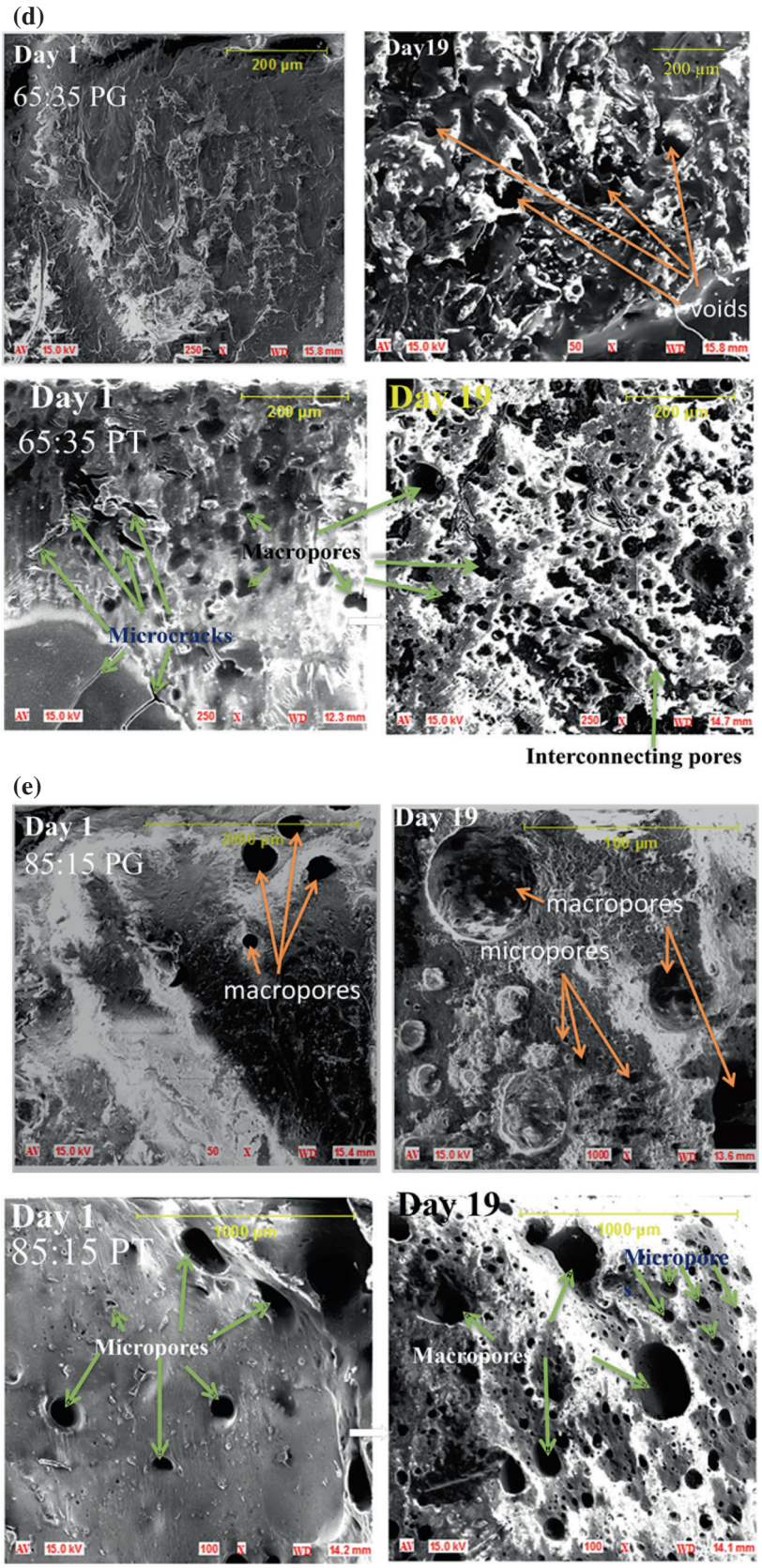

Fig. 1 Continued

Multiple cracks were formed on PLGA-75:25-PT with increasing hydrolysis (Fig.1c (PT)). SEM images of samples (PLGA 65:35 PG/PT, and 85:15 PG/PT) are also compared (Fig. 1d–e).

The porosities of the samples were characterized using the Gwyddion software package (version 2.40). Prior to incubation, the sample loaded with PG (Figs. 1b-65:35 PG) had a rough surface with no evidence of porosity. However, it had pore sizes between 1.2 to50 µm (with a mean pore size of ~10 µm) when incubated for 45 days) as compared with samples loaded with PT (Fig. 1b-65:35 PT), which initially had pore sizes ranging from 0.1 to 1.2 (with a mean pore ~1 µm) and pore sizes between 0.1 to ~20 µm were recorded on day 45 (Fig. 1b-65:35 PT). PLGA 75:25 PT (Fig. 1c) had pore sizes between 0.4 to14.8 µm (mean pore size ~2.54 µm).

The interior of the scaffolds were dominated with macro and micro pores than at the surfaces. The porosities of the PLGA-based minirods are in connection with interfacial diffusion due to the removal of volatile solvents such as DCM, ethanol and DMSO, which were initially used to dissolve the polymers or drugs. The evaporation of the volatile solvents in the formed minirods involves oxygen bubbling through the polymer matrix. This creates micro/macro pores, and the diffusion of the volatile solvents could serve as pore initiators. Pore dominance was found to increase with increasing hydrolysis. This was found to be statistically significant with P-values ≥ 0.05 (Fig. 1d–f). Although the samples loaded with PG and PT were both porous, the samples loaded with PT(1c-75:25PT) showed evidence of micro/macro cracks.

There was a clear relation between the type of drug loaded and porosity. This can be observed in the optical microscopy images (Fig. 1b, c) and the SEM images (Fig. 1d, e). Pore density was high in PLGA-based minirod with PT-loaded (Fig. 1d, e) as compared with PG-loaded minirods. Moreover, there was a clear difference between the observed effects of polymer ratio and porosity. Samples containing high ratios of lactic acid (LA) revealed larger pore areas than those containing lower amounts of LA. By ratio, PLGA 65:35PG (Fig. 1d) had less pore area as compared to PLGA 85:15 PG (Fig. 1d). Similar results were observed in PLGA 65:35PT (Fig. 1d) and PLGA 85:15 PT (Fig. 1e). Hence, the increase in the pore areas within minirods contributes to ~75% of the mean porosity, while pore density contributes about 15–25% to the mean porosity.

3.3 PBS absorption and mass loss

Figure 2a–d presents drug release and mass loss against time. The rates at which PBS diffused (absorption time) into the interior part of PLGA-based minirods were very slow for PT-loaded samples. It took 1–10 days for PG-loaded samples (Fig. 2a–c) to be saturated with PBS (at the peak of the mass loss), whiles for PT-loaded samples; it took 1–50 days (Fig. 2a) and1–90 days (Fig. 2b, c). The uptake of PBS was found to increase with degradation time (hydrolysis) due to an increase in the permeability of the polymer matrix. Porous structures were obtained with porosity becoming more pronounced as a result of degradation products removed over time (Fig. 1a–e). An increase in the content of lactide in PLGA-based minirods also decreased PBS absorption capacity. It, therefore, required longer time in aqueous environment to break the covalent bonds to improve upon the maximum release of drugs. Degradation rates and half-lives of drug release are presented (Table 1). Multipulse drug release showed initial exponential decayed with incubation time (Fig 2a–d). The rates of mass loss in PLGA-PG-based minirods (Figs. 2b–d) were statistically significant. The p-values for PLGA-PG 65:35, 75:25 and 85:15 were 0.082, 0.698 and 0.655, respectively, except for PLGA-50:50 (with $p = 0.046$) (Fig. 3a). A comparison with samples loaded with PT, PLGA 65:35-PT and 75:25-PT, and was also found to be statistically significant (with $p = 0.837$), while the result for PLGA 85:15-PT showed no difference.

3.4 Drug diffusion and reaction rates

The optimum drug release were observed to be:1–30 days for PLGA 65:35-PG and 1–80 days for PLGA 65:35-PT (Fig. 2a); 1–60 days for PLGA 75:25-PG and 1–80 days for PLGA 75:25-PT (Fig. 2b), 1–105 days for PLGA 85:15-PG with 1–110 days for PLGA 85:15-PT (Fig. 2c). There is a clear relation between polymer ratio and the duration of drug release. Moreover, the result (Fig. 3a, b) also indicated an extended drug release from PLGA 85:15-PT as compared to PLGA 65:35-PT and 75:25-PT.

The molecular diffusion of PBS (a biofluid) into the minirods is a function of both the polymer and the biofluid. The overall diffusion in the matrix of the minirods was affected by the morphology of the minirods, the solubility of the minirods in the biofluid, the surface or interfacial energies of the polymer, the molecular size of the drug molecules as well as the molecular weight of the polymer ratio.

Cumulative drug released for PLGA-based minirods are presented (Fig. 3a, b) for samples loaded with PG and PT, respectively. There was initial burst release from the polymer matrices by diffusion. However, the release rates were much slower for PLGA 85:15 PT (Fig. 3a) than the other polymer ratios due to differences in molecular weights.

Drug encapsulation efficiency (DEE) and drug loading content (DL) are presented in Table 2 for PLGA-based minirods. The DEE was between 43 to 92% for

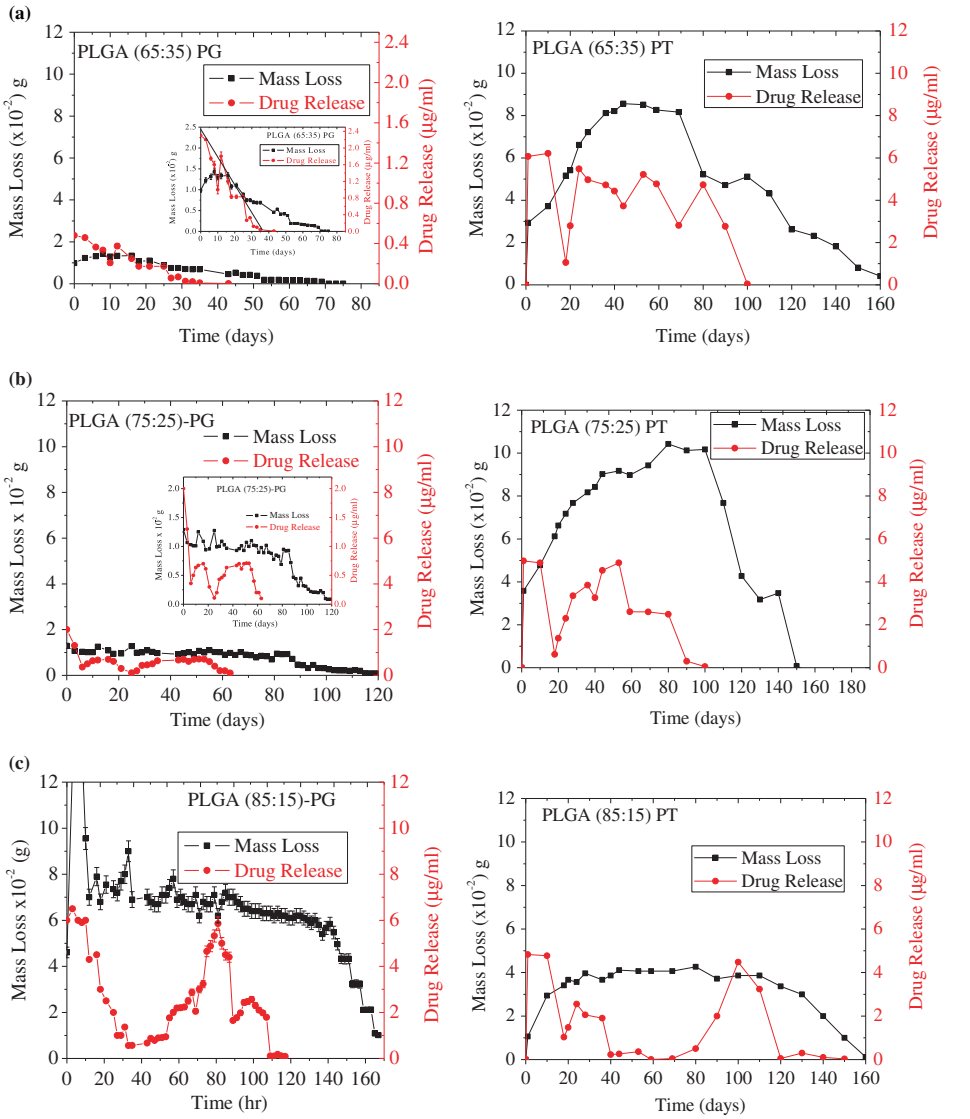

Fig. 2 **a–c** Multi-pulse drug release versus degradation of PLGA-based minirods at 37 °C, pH "7.4", 60 rpm: **a** Comparison of PT and PG minirods (65:35 ratio), **b** Comparison of PT and PG minirods (75:25 ratio) and **c** Comparison of PT and PG minirods (85:15 ratio)

PG-encapsulated minirods, whiles 50 to 89% was the case when PT was encapsulated. The DL for PLGA-PG minirods varied from 2.53–5.43%, while 3.77–4.82% was reported when PT was encapsulated. However, DEE and DL for PLGA-based minirods showed no statistical significance, irrespective of the different polymer ratios or the type of drug encapsulated (Fig. 3a, b and Table 2). The initial diffusion rates for samples encapsulated with PG were between 14.77–25.11 $\times$ 10^{-6} m^2/s, while the diffusion rates for samples encapsulated with PT were between 2.00–22.70 $\times$ 10^{-6} m^2/s.

4 Discussion

The optical microscopy images of the PLGA-based minirods (Fig. 1a–c) indicates that, unlike polymer melting methods [19], the dissolution method of casting has a much better chance of incorporating polymers and drugs into degradable structures. The method also avoids heating effects on the incorporated drugs, while ensuring that the shapes of the structures can be obtained by molding following slight compression. The images obtained on the 36th and 45th days (during in vitro degradation) showed evidence of surface erosion, as well as bulk degradation. Changes in colors were observed due to the removal of drugs and degradable products. This was more pronounced in PLGA 65:35-PG minirods (Fig. 1b). In general, the amorphous regions absorbed PBS quicker, and degraded faster than the crystalline regimes.

Pore areas of the PLGA-based minirods are associated with pore sizes. Increase in the pore size leads to an increase in pore area, hence an increase in the diffusion of solutes. Samples with high mean pore size ranges implies large pore

areas are available in the polymer matrix for the diffusion of drug molecules (out of the polymer) /PBS (into and out of the polymer network) with ease. Moreover, porosity of the minirods is enhanced with an increase in the pore areas and pore densities (the number of pores per unit area) or the combination of the two [37]. Pore areas in the minirods contributed to ~75% of the mean porosity, whiles pore density contributed to 15–20% of the mean porosity. When there are no pores in the body of the minirods, they consist of micro-voids. The voids (micro pores) consist of the gaps between molecular chains. Generally, the optical micrographs of PLGA-PG samples (Fig. 1a, c) were more porous than those loaded with PT, except for the case of Fig. 1e. The result therefore is in agreement with recent study on the synthesis and physico-chemical characterization of biodegradable PLGA-based microparticles loaded with PG and PT [38], which reported porous PG-loaded microspheres as compared to PLGA microspheres loaded with PT formed at similar conditions. For a one dimensional (1-D) drug diffusion equation $\left(L_x = \sqrt{2Dt}\right)$, a linear relationship exist between L_x and $\sqrt{t}$ [34]. This indicates the significant contributions of pore sizes (especially macropores) to enhance the mass flow rate of drugs from the minirods. In otherwise, drugs could be trapped by the polymer matrix, even with high pore density containing micro pores. This result is in agreement with recent work on hydrogels [39].

In terms of polymer ratios, the pore density and sizes were high in polymers with high ratio of lactide units. The higher the content of lactide units to a lesser glycolide ratio, the higher the porosity. Meanwhile, higher content of lactide increases the molecular weight of the polymer. The result shows PLGA with higher molecular weight produces appreciable porous structures (Fig. 1d, e). This result thus agreed with recent work [40]. Despite the high porosity of the minirods for drug to diffuse out of the polymer matrix (Fig. 1e), the degradation rates plays a role in determining drug release kinetics. The higher the content of lactide units, the longer the time required for degradation as compared to samples with large glycolide contents.

Profiles of multi-pulses drug release were observed over time (Fig. 2a–c). This is sometimes preferable to continuous release of drug, which may lead to down-regulation of receptors, or even prevent the development of drug resistance [19]. Hence, a device can be fabricated with programmed delivery to achieve pulsatile drug delivery over an extended time to ensure a programmed off period, followed by a prompt and transient drug release in a cycle until the device is completely degraded [19].

Diffusion and degradation represents the mechanisms of drug release from PLGA-based minirods. Degradation was associated with higher water potential in PBS and the

Table 1 Polymer degradation and drug half-lives at 37 °C in PBS pH "7.4" and 60 rpm

Polymer ratio (PLA:PGA)	Half-lives of polymer (days)	Degradation rate, k (mg/day)	Half-lives of drugs release
Control (50:50)	50	0.832	–
65:35 in PG	70	0.208	6.1
75:25 in PG	130	0.174	4.4
85:15 in PG	170	0.116	3.8
65:35 in PT	85	0.057	4.2
75:25 in PT	152	0.048	4.5
85:15 in PT	180	0.016	2.3

Table 2 Encapsulation efficiencies and drug loading content for PLGA-based minirods

Polymer ratio (PLA:PGA)	Drug encapsulation efficiency (DEE%)	Drug loading content (DL%)
65:35 in PG	82.10	2.53
75:25 in PG	56.20	3.60
85:15 in PG	43.00	5.43
65:35 in PT	89.10	4.82
75:25 in PT	62.10	3.83
85:15 in PT	50.00	3.77

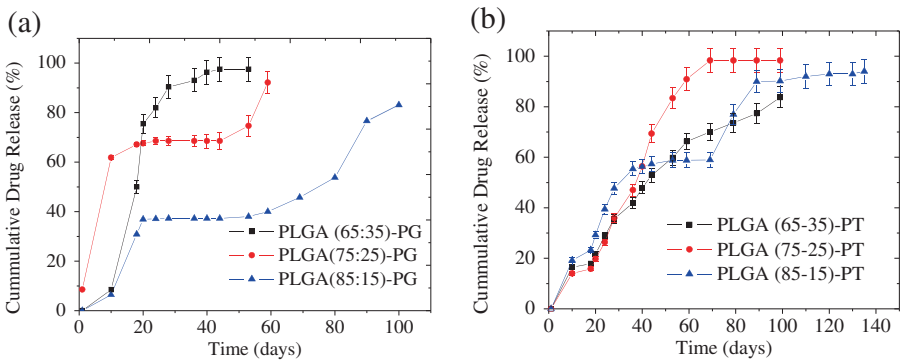

Fig. 3 **a–b** Cumulative drug release from PLGA-based Minirods Incubated at 37 °C, pH "7.4" and under a mechanical agitation of 60 rpm: **a** (PG loaded) and **b** (PT loaded)

penetration of water molecules into the samples (with low water potential). This was followed by hydrolysis of the functional groups and the absorption of water molecules. Further hydrolysis then led to the cleavage of covalent bonds, which causes both surface and bulk erosion.

The degradation of PLGA minirods was dominated by autocatalyzed bulk degradation within the first half of incubation, while surface erosion subsequently sets in via the hydrolysis of ester linkages. Specifically, the degradation of PLGA-PG minirods was largely associated with surface erosion from the surfaces of the samples (Fig.1a–e). The rates of mass loss were also faster than the ingress of PBS/water into the bulk samples (Fig. 2a–c, graphs on *left*). On the other hand, PLGA-PT exhibited a dominance of bulk degradation, which occured throughout the whole samples (Fig.1a–e), whereby the ingress of water molecules was faster than the rate of polymer degradation (Fig. 2a–c, graphs on *right*). This is consistent with the increase in the absorption of PBS, for PLGA-PT-loaded samples, especially PLGA 65:35 PT and 75:25 PT (Fig. 2a–b, graphs on *right*). The degradation kinetics of PLGA-based microparticles (loaded with PG and PT) in previous study [38] indicates heterogeneous networks on the matrices of the microparticles. The PLGA-based minirods (loaded with PG and PT) as well also reveals heterogeneous networks during degradation in PBS. The heterogeneous features from the optical micrographs coupled with the SEM images can then be attributed to an autocatalyzed bulk degradation process [38].

The crystallinity, presence of chain defects, molecular weight, intake of PBS, increase in glycolide content, type of drug loaded, including other intrinsic properties, affects the rates of the in vitro degradation of the minirods. However, earlier reports indicate the physico-chemical properties of the drugs loaded as well as the interaction between drugs, and polymer matrix stands to be a critical factor that can hinder polymer degradation and drug release [41]. These studies revealed a long range release of drugs from PLGA-PT samples as compared to those from PLGA-PG. This is in agreement with previous studies, [42] which indicate hydrophilic drugs facilitate water penetration in the polymer, and subsequently lead to the creation of a porous polymer networks during drug escape which accelerates polymer degradation. Thus, hydrophobic drug such as PT hindered water diffusion into the polymer matrix, and therefore retard its degradation. Factors influencing polymer-drug degradation have been extensively reviewed [43].

The release of PG from PLGA-based composites can be tuned with multi-pulsed delivery to deliver PG over an extended period of time. The tuning can be engineered by relating erosion and the mechanism of drug release to the drug release kinetics. In vivo experiments are therefore needed to ascertain the in vitro results. This is clearly, a challenge for future work.

4.1 Summary and concluding remarks

Drug release kinetics and polymer degradation mechanisms were studied to provide insights for the design of implantable biodegradable devices for localized cancer treatment. The first stages of hydrolysis started with water molecules from PBS penetrating deeply into the polymers. The water molecules caused the functional groups in the polymer chains to hydrolyze and absorb the PBS by natural diffusion , resulting in the cleavage of chemical bonds. The resulting release of degradable products led to mass loss, which is a characteristic of polymer erosion.

The studies revealed a long range release of drugs from PLGA-PT compared to those from PLGA-PG. However, the samples containing PT were hard and brittle. They also fractured easily resulting in loss of the geometry or shape. In contrast, drug release and degradation were faster in PLGA loaded with PG. The PLGA samples loaded with PG were also soft and flexible. PLGA-PG are potential scaffolds for implantable cancer drug delivery devices than PLGA-PT samples. The drug release characteristics were associated with polymer degradation and erosion mechanisms that were revealed by microscopic observations at different stages of drug release.

Acknowledgements The authors are very grateful to the World Bank African Centres of Excellent Project (Pan-African Materials Institute (PAMI) with grant No. P126974), the African Capacity Building Foundation with Grant No. 292, Princeton University School of Engineering and Applied Sciences (SEAS) and the Worcester Polytechnic Institute for financial support. The authors are also grateful to the Nelson Mandela Institute (NMI) and the African University of Science and Technology (AUST) for the scholarships given to the students. Appreciation is also extended to Prof. Eric Garfunkel and Dr. Adeoye Soyemi for useful technical discussions.

Compliance with ethical standards

Conflict of interest The authors declare that they have no competing interests.

References

1. Alwan A. Global status report on noncommunicable diseases in 2010. Geneva: World Health Organization; 2011. p. 164
2. Ferlay J, Shin HR, Bray F, Forman D, Mathers CD, Parkin DM. Estimates of worldwide burden of cancer in 2008: GLOBOCAN 2008. Int J of Cancer. 2010;127:2893–917.
3. Mathers DC, Loncar D. Updated projections of global mortality and burden of disease, 2002–2030; data sources, methods and results. Geneva, Switzerland: World Health Organization; 2005. p. 6.
4. Borgstede JP, Bagrosky BM. Early diagnosis and treatment of cancer series: breast cancer: screening of high-risk patients. Philadelphia: Saunders Elsevier; 2011.
5. Pisano ED, Gatsonis C, Hendrick E, Yaffe M, Baum JK, Acharyya S, Conant EF, Fajardo LL, Bassett L, D'Orsi C, Jong R,

Rebner M. Diagnostic performance of digital versus film mammography for breast-cancer screening. N Engl J Med. 2005;353:1773–83.
6. Saslow D, Boetes C, Burke W, Harms S, Leach MO, Lehman CD, Morris E, Pisano E, Schnall M, Sener S, Smith RA, Warner E, Yaffe M, Adrews KS, Russell CA. American cancer society guidelines for breast screening with MRI as an adjunct to mammography. CA Cancer J Clin. 2007;57:75–89.
7. Smith RA, Saslow D, Sawyer KA, Burke W, Costanza ME, Evans WP III, Foster RS, Hendrick E, Eyre HJ, Sener S. American cancer society guidelines for breast cancer screening. CA Cancer J Clin. 2003;53:141–69.
8. Breast Cancer Signs & Symptoms. In: Early symptoms. What health, healthy living for everybody. 2016. http://www.whathealth.com/breastcancer/symptoms.html. Accessed 15 Dec 2016.
9. David N, Mark WD. The development and testing of a new temperature-sensitive drug delivery system for the treatment of solid tumors. Adv Drug Deliv Rev. 2001;53:285–305.
10. Hildebrandt B, Wustin P, Ceelen WP. Peritoneal carcinomatosis: a multidisciplinary approach. New York, NY: Springer; 2007.
11. Oni Y, Theriault C, Hoek AV, Soboyejo WO. Effects of temperature on diffusion from PNIPA-based gels in a BioMEMS device for localized chemotherapy and hyperthermia. Mater Sci Eng C. 2011;31:67–76.
12. Oni Y, Soboyejo WO. Swelling and diffusion of pnipa-based gels for localized chemotherapy and hyperthermia. Mater Sci Eng C. 2012;32:24–30.
13. Kavanagh BD, Timmerman RD. Stereotactic body radiation therapy. 1st ed. Philadelphia: Lippincott Williams & Wilkins; 2004.
14. Del Regato JA. Radiological oncologists: the unfolding of a medical specialty. Reston (VA): Radiology Centennial Inc., University of Michigan, USA; 1993;268: 167–76.
15. Xu M, Qian J, Liu X, Liu T, Wang H. Stimuli-responsive pegylated prodrugs for targeted doxorubicin delivery. Mater Sci Eng C. 2015;50:341–47.
16. Danyuo Y, Ani CJ, Obayemi JD, Dozie-Nwachukwu S, Odusanya OS, Oni Y, Anuku N, Malatesta K, Soboyejo WO. Advanced Materials for Sustainable Development. In: Soboyejo W, Odusanya S, Kana Z, Anukwu N, Malatesta K, Dauda M, editors. Prodigiosin release from an implantable biomedical device: effect on cell viability. Switzerland: Trans Tech Publications; 2016. p. 3–18.
17. Uhrich KE, Cannizzaro SM, Langer RS, Shakesheff KM. Polymeric systems for controlled drug release. Chem Rev. 1999;99:3181–98.
18. Danyuo Y, Obayemi JD, Dozie-Nwachukwu S, Ani CJ, Odusanya OS, Oni Y, Anuku N, Malatesta K, Soboyejo WO. Prodigiosin release from an implantable biomedical device: kinetics of localized cancer drug release. J Mater Sci Eng C. 2014;42(1):734–45.
19. Makadia HK, Siege SJ. Poly lactic-co-glycolic acid (PLGA) as biodegradable controlled drug delivery carrier. Polymers (Basel). 2011;3(3):1377–97.
20. Allison SD. Effect of structural relaxation on the preparation and drug release behavior of poly(lactic-co-glycolic)acid microparticle drug delivery systems. J Pharm Sci. 2008;97:2022–35.
21. Mundargi R, Babu V, Rangaswamy V, Patel P, Aminabhavi T. Nano/micro technologies for delivering macromolecular therapeutics using poly(D,L-lactide-co-glycolide) and its derivatives. J Cont Rel. 2008;125:193–209.
22. Mohamed F, van der Walle CF. Engineering biodegradable polyester particles with specific drug targeting and drug release properties. J Pharm Sci. 2008;97:71–87.
23. Metters AT, Bowman CN. A statistical kinetic model for the bulk degradation of PLA-b-PEG-b-PLA hydrogel networks; incorporating network non-idealities. J Phys Chem B. 2001;104:8069–76.
24. Obayemi JD, Danyuo Y, Dozie-Nwachukwu S, Odusanya OS, Anuku N, Malatesta K, Yu W, Uhrich KE, Soboyejo WO. PLGA-based microparticles loaded with bacterial-synthesized prodigiosin for anticancer drug release: effects of particle size on drug release kinetics and cell viability. Mater Sci Eng C. 2016;66:51–65.
25. Behravesh E, Yasko AW, Engel PS, Mikos AG. Synthetic biodegradable polymers for orthopaedic applications. Clin Orthop Relat Res. 1999;367:118–25.
26. Middleton E Jr., Kandaswami C, Theoharide TC. The effects of plant flavonoids on mammalian cells: implications for inflammation, heart disease and cancer. Pharmacol Rev. 2000;52 (4):673–751.
27. Park TG. Degradation of poly (D,L-lactic acid) microspheres: effect of molecular weight. J Control Release. 1994;30:161–73.
28. Metzmacher I, Radu F, Bause M, Knabner P, Friess W. A model describing the effect of enzymatic degradation on drug release from collagen minirods. Eur J Pharm Biopharm. 2007;67 (2):349–60.
29. Danyuo Y, Dozie-Nwachukwu S, Obayemi JD, Ani CJ, Odusanya OS, Oni Y, Anuku N, Malatesta K, Soboyejo WO. Swelling of poly(N-isopropyl acrylamide) (PNIPA)-based hydrogels with bacterial-synthesized prodigiosin for localized cancer drug delivery. Mater Sci Engr C. 2016;59:19–29.
30. Flanagan RJ, Taylor AA, Watson ID, Whelpton R. Fundamentals of analytical toxicology. Newyork, USA: Wiley and Sons; 2007. p. 1–486.
31. Pathiraja AG, Raju A. Biodegradable synthetic polymers for tissue engineering. Eur Cell Mater. 2003;6:1–16.
32. Koleske JV. Blends containing poly(∈-caprolactone) and related polymers. In: Paul R, Newman S, editors. Polymer Blends. New York, NY: Academic; 1978. p. 369–89.
33. Peppas AN. Analysis of fickian and non-fickian drug release from polymers. Pharm Acta Helv. 1985;60(4):110–11.
34. Danyuo Y, Obayemi JD, Dozie-Nwachukwu S, Ani CJ, Odusanya OS, Oni Y, Anuku N, Malatesta K, Soboyejo WO. Prodigiosin release from an implantable biomedical device: kinetics of localized cancer drug release. Mater Sci Eng C. 2014;42(1):734–45.
35. Ogunnaike BA. Random phenomena, fundamentals of probability & statistics for engineers. Newark: University of Delaware; 2009.
36. McDonald JH. Handbook of biological statistics. 3rd ed. Maryland: Sparky House Publishing; 2014.
37. Thomas CDL, Feik SA and Clement JG. Increase in pore area, and not pore density, is the main determinant in the development of porosity in human cortical bone. J Anat. 2006;209:219–30.
38. Obayemi JD, Danyuo Y, Dozie-Nwachukwu S, Odusanya OS, Anuku N, Malatesta K, Yu W, Uhrich KE, Soboyejo WO. PLGA-based microparticles loaded with bacterial-synthesized prodigiosin for anticancer drug release: effects of particle size on drug release kinetics and cell viability. Mater Sci Eng C. 2016;66:51–65.
39. Tamagawa H, Popovic S, Taya M. Pores and diffusion characteristics of porous gels. Polymer. 2000;41:7201–7.
40. Bae SE, Sona JS, Parka K, Han DK. Fabrication of covered porous PLGA microspheres using hydrogen peroxide for controlled drug delivery and regenerative medicine. J Control Release. 2009;133(1):37–43.
41. Chen J, Lee J-W, Hernandez de Gatica NL, Burkhardt CA, Hercules DM, Gardella JA Jr. Time-of-flight secondary ion mass spectrometry studies of hydrolytic degradation kinetics at the surface of poly(glycolic acid). Macromolecules. 2000;33:4726–32.
42. Klose D, Siepmann F. PLGA-based drug delivery systems: importance of the type of drug and device geometry. Int J Pharm. 2008;354:95–103.
43. Engineer C, Parikh J, Raval A. Review on hydrolytic degradation behavior of biodegradable polymers from controlled drug delivery system. Trends Biomater Artif Organs. 2011;25(2):79–85.